

# A High-Temperature Multinuclear NMR Study of $\text{Na}_3\text{AlF}_6\text{--FeO}$ and $\text{Na}_3\text{AlF}_6\text{--Fe}_2\text{O}_3$ Melts

František Šimko,<sup>\*,[a]</sup> Aydar Rakhmatullin,<sup>[b]</sup> Miroslav Boča,<sup>[a]</sup> Vladimír Daněk,<sup>[a]</sup> and Catherine Bessada<sup>[b]</sup>

**Keywords:** Electrolysis / NMR spectroscopy / Cryolitic melts / Aluminium / Iron

In the Hall–Héroult process for the industrial production of aluminum, iron oxide impurities are known to lower the current efficiency as well as the metal quality. Iron can be present in the di- or trivalent form. The nature of dissolved  $\text{Fe}^{\text{III}}$  and  $\text{Fe}^{\text{II}}$  species and the reactions taking place in cryolitic melts have been investigated by high-temperature NMR spectroscopy. The evolution of  $^{27}\text{Al}$ ,  $^{23}\text{Na}$ , and  $^{19}\text{F}$  NMR chemical shifts are reported in the  $\text{Na}_3\text{AlF}_6\text{--FeO}$  and  $\text{Na}_3\text{AlF}_6\text{--Fe}_2\text{O}_3$  systems for different iron oxide contents. They express the formation of oxofluoroaluminate species. For the  $\text{Na}_3\text{AlF}_6\text{--FeO}$  system, the  $^{19}\text{F}$  signal appears only after 14 minutes at 1020 °C. The line position is shifted with

heating time. This evolution is associated with a narrowing of the  $^{27}\text{Al}$  signal due to a decrease in the content of paramagnetic compounds in the sample. This effect is probably caused by the evaporation of an  $\text{Fe}^{\text{II}}$  compound, as already mentioned in the literature. For the  $\text{Na}_3\text{AlF}_6\text{--Fe}_2\text{O}_3$  system we have never observed the  $^{19}\text{F}$  NMR spectra over the full heating time (ca. 30 min). This could be due to the influence of paramagnetic  $\text{Fe}^{\text{III}}$  nuclei, probably in  $\text{FeF}_6^{3-}$  species present in the melt.

(© Wiley-VCH Verlag GmbH & Co. KGaA, 69451 Weinheim, Germany, 2006)

## Introduction

Aluminum is produced industrially by the Hall–Héroult electrolytic process. The impurities present during the process represent a critical problem because they negatively influence the current efficiency and may lower the metal quality.<sup>[1,2]</sup> Iron is one of the predominant impurities in the industrial production and can be present in the di- or trivalent state, especially as oxides ( $\text{FeO}$ ,  $\text{Fe}_2\text{O}_3$ ). Iron is introduced with the raw materials and/or by corrosion of the different cell parts. The nature of the dissolved species and different reactions taking place upon dissolution of  $\text{Fe}_2\text{O}_3$  and  $\text{FeO}$  into cryolite (the major component of the electrolyte) is a crucial question. Because of the experimental difficulties due to the corrosive properties of fluoride melts at high temperature, only a few data have been reported, mainly deduced from solubility measurements.<sup>[3–9]</sup> From cryoscopy measurements, Diep<sup>[5]</sup> has suggested that  $\text{Fe}_2\text{O}_3$  dissolves in cryolite to form nonvolatile sodium hexafluoroferrite ( $\text{Na}_3\text{FeF}_6$ ), while for  $\text{Fe}^{\text{II}}\text{O}$  the formation of  $\text{Na}_x\text{FeF}_{(2+x)}$  complexes has been assumed by Jentofsen.<sup>[8,9]</sup> In both systems, the formation of oxofluoroaluminate complexes ( $\text{Al}_2\text{OF}_6^{2-}$  and  $\text{Al}_2\text{O}_2\text{F}_4^{2-}$ ) has also been proposed

depending on the iron oxide concentration in the melt. Up to now, no direct detection of the ionic species formed in both kinds of melts has been attempted. Therefore, we propose in this paper to present their in situ NMR description. This spectroscopy is sensitive to the local environment around a selected nucleus, therefore it allows both qualitative and quantitative information about the different species existing in the bath to be determined.<sup>[10,11]</sup> The presence of  $\text{Fe}^{\text{II}}$  in the melts can cause some paramagnetic effects on the NMR signal of the different nuclei, mainly broadening and shift and shape distortion of the line. These effects can be large enough to dramatically decrease the signal intensity and make any observation impossible. We will try to take advantage of this interaction and its effects on the spectra that we can associate with the detection of  $\text{Fe}^{\text{II}}$  formation in the melt, and its implication on the ionic species.

We report in this paper  $^{27}\text{Al}$ ,  $^{23}\text{Na}$ , and  $^{19}\text{F}$  NMR measurements at high temperature in the  $\text{Na}_3\text{AlF}_6\text{--FeO}$  and  $\text{Na}_3\text{AlF}_6\text{--Fe}_2\text{O}_3$  binary systems. The combination of the structural information given by the NMR signal of the different nuclei enables us to give the first experimental evidence of the formation of new species due to dissolution of iron oxide in these high-temperature melts.

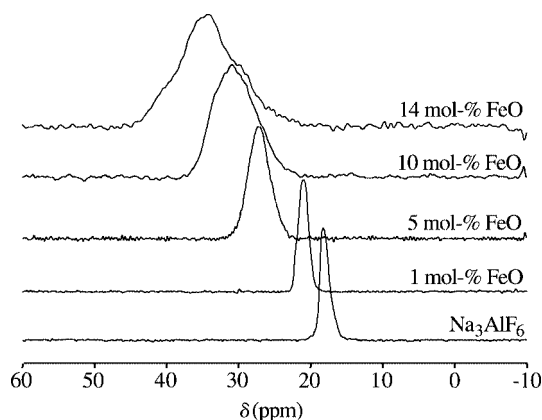
## Results and Discussion

### $^{27}\text{Al}$ NMR Spectra

The HT  $^{27}\text{Al}$  NMR spectra of molten  $\text{Na}_3\text{AlF}_6$  with different amounts of  $\text{FeO}$  are shown in Figure 1.

[a] Institute of Inorganic Chemistry, Slovak Academy of Sciences, Dúbravská cesta 9, 84536 Bratislava, Slovakia  
E-mail: uachsim@savba.sk  
Fax: +421-2-5941-0444

[b] Centre de Recherches sur les Matériaux à Haute Température CNRS,  
1D av. de la Recherche Scientifique, 45071 Orléans, France

Figure 1. HT  $^{27}\text{Al}$  NMR spectra of  $\text{Na}_3\text{AlF}_6\text{-FeO}$  melts at 1020 °C.

Because of the dynamics existing in the melt, and the rapid exchange between the different possible species involving the nucleus under observation, all the HT NMR spectra consist of a single Lorentzian-shaped line. In pure cryolite, a sharp line at  $\delta = 18.3$  ppm is observed, in good agreement with the value reported by Lacassagne et al.<sup>[11]</sup> Upon addition of FeO the signal is shifted towards higher chemical shifts and broadens progressively with increased FeO content. For 1 mol-% added FeO, the line position is moved slightly to  $\delta = 21$  ppm, and the linewidth is unchanged. For 14 mol-% FeO, however, the peak is centered at  $\delta = 34$  ppm with an important modification of the line-shape ( $\Delta_{1/2} = 900$  Hz; Table 1). We observe the same kind of evolution for very low  $\text{Fe}_2\text{O}_3$  additions (Figure 2), with a shift of 7 ppm for 1 mol-% added  $\text{Fe}_2\text{O}_3$ .

Table 1. Composition,  $^{27}\text{Al}$  and  $^{23}\text{Na}$  NMR chemical shifts, and linewidths in  $\text{Na}_3\text{AlF}_6\text{-FeO}$  and  $\text{Na}_3\text{AlF}_6\text{-Fe}_2\text{O}_3$  melts at 1020 °C.

$x(\text{FeO})$ [mol-%]	$\delta(^{27}\text{Al})$ [ppm]	$\Delta_{1/2}$ [Hz]	$\delta(^{23}\text{Na})$ [ppm]	$\Delta_{1/2}$ [Hz]
0.0	18.8	149	-6.5	130
1	21.0	179	-6.4	179
5	27.3	398	—	—
10	30.9	765	—	—
14	34.3	903	—	—

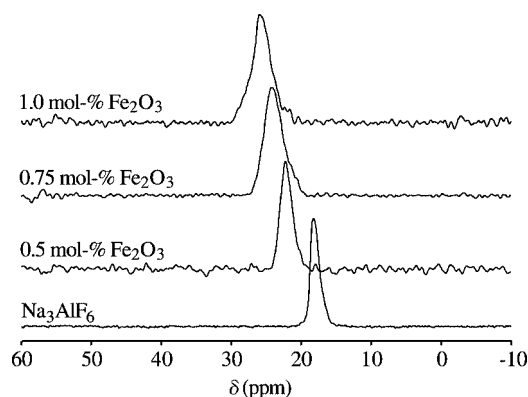
  

$x(\text{Fe}_2\text{O}_3)$ [mol-%]	$\delta(^{27}\text{Al})$ [ppm]	$\Delta_{1/2}$ [Hz]	$\delta(^{23}\text{Na})$ [ppm]	$\Delta_{1/2}$ [Hz]
0.0	18.8	149	-6.5	130
0.5	22.2	256	-5.5	199
0.75	24.2	326	-5.0	262
1	26.0	361	-4.8	296

These shifts can be caused by a) a modification in the local environment of the aluminum nucleus and the formation of new aluminum species with higher chemical shifts and b) the existence of unpaired electrons in the system that affect the local magnetic field around the observed nucleus and cause a shift and broadening of the line.

Let us discuss the first point. In the liquid phase, the observed peak position is the average of the chemical shifts of individual species present in the melt weighted by their respective populations [Equation (1)] and  $\sum_i X^{\text{Al}}(A_i) = 1$ .

$$\delta^{\text{Al}}_{\text{mes}} = \sum_i X^{\text{Al}}(A_i) \cdot \delta^{\text{Al}}(A_i) \quad (1)$$

Figure 2. HT  $^{27}\text{Al}$  NMR spectra of  $\text{Na}_3\text{AlF}_6\text{-Fe}_2\text{O}_3$  melts at 1020 °C.

where  $X^{\text{Al}}(A_i)$  is the atomic fraction of Al atoms in the  $A_i$  species and  $\delta^{\text{Al}}(A_i)$  its chemical shift.

The  $^{27}\text{Al}$  chemical shift range for aluminum in oxide and fluoride materials is known to correlate strongly with the nature and number of the nearest neighbors around the aluminum atom and thus to its coordination. For  $\{\text{AlO}_4\}$  tetrahedral sites in oxides the  $\delta$  values fall in the range  $\delta = 55$  to 90 ppm and in the range  $\delta = -20$  to +20 ppm for the  $\{\text{AlO}_6\}$  octahedral sites.  $\{\text{AlO}_5\}$  groups have been characterized in different aluminosilicate structures with  $\delta$  values of about 30 to 40 ppm. In fluorides, significantly different chemical shift ranges have also been reported for  $\text{AlF}_4^-$ ,  $\text{AlF}_5^{2-}$ , and  $\text{AlF}_6^{3-}$  units. They are clearly shifted towards lower chemical shifts:  $\delta = 4$  to -15 ppm for  $\text{AlF}_6^{3-}$ ,  $\delta = 40$  to 35 ppm for  $\text{AlF}_4^-$ , and around  $\delta = 20$  ppm for  $\text{AlF}_5^{2-}$  (Table 2).<sup>[10]</sup>

Table 2.  $^{27}\text{Al}$  chemical shift ranges for Al-O and Al-F coordination.<sup>[11]</sup>

Al coordination	$\delta(^{27}\text{Al})$ [ppm]
$\text{AlO}_4$	90–55
$\text{AlO}_5$	40–30
$\text{AlO}_6$	20 to -20
$\text{AlF}_4$	35–40
$\text{AlF}_5$	20
$\text{AlF}_6$	4 to -15

These chemical-shift ranges will help us to better understand the chemical-shift evolution measured in the melts. An increase of the  $^{27}\text{Al}$  chemical shift can thus be related to a decrease of the average coordination number of the aluminum atoms and the formation of species with a lower coordination number.

It is also expected that the addition of oxides ( $\text{Al}_2\text{O}_3$ , FeO,  $\text{Fe}_2\text{O}_3$ ) to molten cryolite will result in the formation of oxygen-containing entities, the most probable being the oxofluoroaluminate species  $\text{Al}_2\text{OF}_6^{2-}$  and  $\text{Al}_2\text{O}_2\text{F}_4^{2-}$  depending on the oxide content. From an NMR point of view, the local configuration around the aluminum atom in each of these two anions corresponds to tetrahedral environments  $\{\text{AlOF}_3\}$  and  $\{\text{AlO}_2\text{F}_2\}$ . Lacassagne et al.<sup>[11]</sup> have determined the  $^{27}\text{Al}$  chemical shifts of these species as  $\delta^{\text{Al}}_{\text{Al}_2\text{OF}_6^{2-}} = 50.0 \pm 0.5$  ppm and  $\delta^{\text{Al}}_{\text{Al}_2\text{O}_2\text{F}_4^{2-}} =$

58.5 ± 0.5 ppm, which lie between the chemical-shift ranges of {AlO<sub>4</sub>} and {AlF<sub>4</sub>} tetrahedral units. The formation of such oxofluoroaluminate species in the melt by dissolution of iron oxides should thus contribute to an increase of the measured <sup>27</sup>Al chemical shifts in molten cryolite, where aluminum atoms are essentially involved in pure fluoride environments.

Because of the line-shape distortion observed for high FeO amounts it is difficult to interpret the position of the line unambiguously. This distortion can be assigned to a paramagnetic effect that causes a line broadening and should certainly contribute to the shift of the line observed.

Iron in the +2 and +3 oxidation states may exist in a low-spin or a high-spin state, depending on the ligand-field strength. In both systems, F<sup>−</sup> and O<sup>2−</sup> ligands create a rather soft ligand field.<sup>[12]</sup> Thus, the high-spin state will be preferred [(t<sub>2g</sub>)<sup>4</sup>(e<sub>g</sub>)<sup>2</sup> for Fe<sup>II</sup> and (t<sub>2g</sub>)<sup>3</sup>(e<sub>g</sub>)<sup>2</sup> for Fe<sup>III</sup>]. This is also supported by the increasing Boltzman distribution of the higher states with temperature increase. The important line broadening indicates that the distribution of local magnetic fields is spread over the sample. The broadening of the resonance signal reflects the extent of interaction between the unpaired electrons and the nucleus.<sup>[13]</sup>

We can calculate the <sup>27</sup>Al chemical shifts in the Na<sub>3</sub>AlF<sub>6</sub>–10 mol-% FeO system, by taking into account only the aluminum species involved in the suggested reaction (A).



At this FeO concentration, the Al<sub>2</sub>O<sub>2</sub>F<sub>4</sub><sup>2−</sup> anion is supposed to be formed in the melt in addition to the fluoroaluminate species AlF<sub>6</sub><sup>3−</sup>, AlF<sub>5</sub><sup>2−</sup>, and AlF<sub>4</sub><sup>−</sup> due to a dissociation reaction of unreacted molten cryolite.<sup>[1,14–18]</sup> Thus, starting from 90 mol of Na<sub>3</sub>AlF<sub>6</sub> and 10 mol of FeO, we assume the formation of 5 mol of Al<sub>2</sub>O<sub>2</sub>F<sub>4</sub><sup>2−</sup> by reaction with 10 mol of Na<sub>3</sub>AlF<sub>6</sub>. After the reaction our system would contain 5 mol of Al<sub>2</sub>O<sub>2</sub>F<sub>4</sub><sup>2−</sup> and 80 mol of unreacted Na<sub>3</sub>AlF<sub>6</sub>.

From the mass-balance equation expressed for aluminum, we can calculate the anionic molar fractions of the different species in the melt.  $x_i = \frac{N_i}{N_T}$ , where  $N_i$  is the number of mols of the species  $i$  and  $N_T$  the total number of mols. The atomic fractions can then be easily deduced and substituted in Equation (2) to give Equation (1).

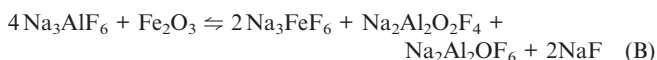
$$\delta_{\text{Al}}^{27}(\text{calcd.}) [\text{ppm}] = 0.0588 \cdot \delta_{\text{Al}}^{27}(\text{Al}_2\text{O}_2\text{F}_4^{2-}) + 0.9412 \cdot \delta_{\text{Al}}^{27}\left(\sum_{x=4}^6 \text{AlF}_x^{(x-3)-}\right) \quad (2)$$

In this calculation, the contribution of unpaired electrons is not taken into account.  $\delta_{\text{Al}}^{27}\left(\sum_{x=4}^6 \text{AlF}_x^{(x-3)-}\right) = 18.8$  ppm is the chemical shift measured in molten cryolite, and  $\delta_{\text{Al}}^{27}(\text{Al}_2\text{O}_2\text{F}_4^{2-}) = 58.5$  ppm is the <sup>27</sup>Al chemical shift value reported by Lacassagne et al.<sup>[11]</sup> for the Al<sub>2</sub>O<sub>2</sub>F<sub>4</sub><sup>2−</sup> species. This gives Equation (3).

$$\delta_{\text{Al}}^{27}(\text{calcd.}) [\text{ppm}] = 0.0588 \times 58.5 + 0.9412 \times 18.8 = 21.1 \quad (3)$$

This calculated value is different from the experimental chemical shift measured in the melt of  $\delta = 30.9$  ppm. This difference can be associated with the presence of the unpaired electrons of iron in the oxidation state +2, as mentioned above.

In the (Na<sub>3</sub>AlF<sub>6</sub>–Fe<sub>2</sub>O<sub>3</sub>) system the formation of two oxofluoroaluminate anions should be considered even at such a low iron oxide content according to reaction B.<sup>[18,19]</sup>



Addition of 1 mol of Fe<sub>2</sub>O<sub>3</sub> to cryolite results in the formation of 1 mol of Al<sub>2</sub>OF<sub>6</sub><sup>2−</sup> and 1 mol of Al<sub>2</sub>O<sub>2</sub>F<sub>4</sub><sup>2−</sup> by reaction with 4 mols of Na<sub>3</sub>AlF<sub>6</sub>. After the reaction, the system contains 1 mol of Al<sub>2</sub>OF<sub>6</sub><sup>2−</sup>, 1 mol of Al<sub>2</sub>O<sub>2</sub>F<sub>4</sub><sup>2−</sup>, and 95 mols of unreacted Na<sub>3</sub>AlF<sub>6</sub> and other species that do not contain Al atoms and thus that will not contribute to the <sup>27</sup>Al chemical shift. Normalization gives Equations (4) and (5).

$$\delta_{\text{Al}}^{27}(\text{calcd.}) [\text{ppm}] = 0.0103 \cdot \delta_{\text{Al}}^{27}(\text{Al}_2\text{O}_2\text{F}_4^{2-}) + 0.9794 \cdot \delta_{\text{Al}}^{27}\left(\sum_{x=4}^6 \text{AlF}_x^{(x-3)-}\right) \quad (4)$$

$$\delta_{\text{Al}}^{27}(\text{calcd.}) [\text{ppm}] = 0.0103 \times 50 + 0.0103 \times 58 + 0.9794 \times 18.3 = 19.0 \quad (5)$$

The difference between the calculated and the experimental chemical shift of  $\delta = 26.0$  ppm can again be attributed to the presence of unpaired electrons of iron in the oxidation state +3.

## <sup>23</sup>Na NMR Spectra

No significant modifications of the <sup>23</sup>Na chemical shift were observed in both systems. In the Na<sub>3</sub>AlF<sub>6</sub>–FeO system, when the amount of FeO is increased, the line is enlarged and distorted. This indicates the proximity of a paramagnetic element to the <sup>23</sup>Na surroundings but no direct bonding in a defined ionic species.

## <sup>19</sup>F NMR Spectra

No <sup>19</sup>F NMR signal was detected on melting. This can be explained by the existence of a strong paramagnetic effect that can disturb the signal and make it disappear. For Na<sub>3</sub>AlF<sub>6</sub>–10 mol-% FeO a small <sup>19</sup>F signal was observed but only after 14 minutes of heating. This means that some reaction has started that changes the local environment around the fluorine atoms.

In order to follow the kinetics of the dissolution of iron oxides in both systems, NMR spectra were recorded successively for the <sup>27</sup>Al and <sup>19</sup>F nuclei during 30 minutes at 1020 °C.

The evolution of the <sup>19</sup>F NMR spectra of the Na<sub>3</sub>AlF<sub>6</sub>–10 mol-% FeO mixture at 1020 °C is shown in Figure 3 as a function of time. When the heating duration is increased the position and the shape of the signal are modified. The signal position moves towards the position measured in

pure cryolite and at the same time the line becomes narrower (Table 3). This evolution can be explained by a continuous evolution of the nucleus shielding due to a decrease of the concentration of paramagnetic compounds in the investigated sample.

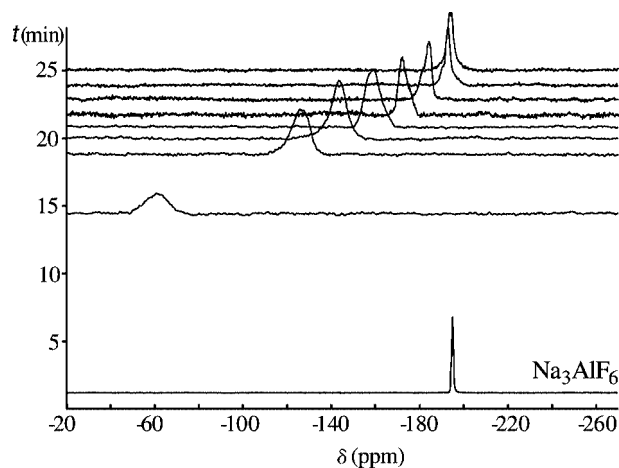


Figure 3. HT  $^{19}\text{F}$  NMR spectra of  $\text{Na}_3\text{AlF}_6$ -10 mol-% FeO at 1020 °C vs. heating time.

Table 3. Time dependence of  $^{27}\text{Al}$  and  $^{19}\text{F}$  signal position ( $\delta$ ) and linewidth ( $\Delta_{1/2}$ ) in the  $\text{Na}_3\text{AlF}_6$ -10 mol-% FeO and  $\text{Na}_3\text{AlF}_6$ -1 mol-%  $\text{Fe}_2\text{O}_3$  systems at 1020 °C.

$\text{Na}_3\text{AlF}_6$ -FeO			$\text{Na}_3\text{AlF}_6$ - $\text{Fe}_2\text{O}_3$		
$t$	$\delta(^{27}\text{Al})$	$\Delta_{1/2}$	$t$	$\delta(^{19}\text{F})$	$\Delta_{1/2}$
[min]	[ppm]	[Hz]	[min]	[ppm]	[Hz]
4	30.9	762	6	—	—
7	31.2	1052	11	—	—
12	31.5	717	14	-61.5	9618
16	27.6	394	19	-126.2	2100
20	22.8	302	20	-145.2	1859
25	22.6	488	21	-160.5	1835
30	23.2	441	22	-172.0	1494
31	23.2	475	23	-184.4	1183
			24	-193.1	971
			25	-194.8	829

The decreasing concentration of paramagnetic iron in the sample is probably caused by the volatilization of  $\text{Fe}^{\text{II}}$  compounds from the melt. The solidified sample was investigated by X-ray diffraction and no crystalline phase containing iron was detected. This confirms the formation of volatile compounds of the type  $\text{Na}_x\text{FeF}_{2+x}$  ( $x = 1, 2$ ),<sup>[19,20]</sup> as already proposed in the literature.<sup>[8,9]</sup>

The same kind of measurements were made for the second system with  $\text{Fe}_2\text{O}_3$  oxide ( $\text{Na}_3\text{AlF}_6$  + 1 mol-%  $\text{Fe}_2\text{O}_3$ ). In this case we were not able to observe any  $^{19}\text{F}$  signal even after more than 30 minutes in the melt. The non-observation of the  $^{19}\text{F}$  signal suggests the presence of stable, non-volatile fluoride species in the melt involving the paramagnetic nuclei, probably in the form of  $\text{FeF}_6^{3-}$  ions.<sup>[5,19]</sup> The paramagnetic effect seems to be strong enough to strongly affect the signal detection.

In the case of  $^{27}\text{Al}$  in  $\text{Na}_3\text{AlF}_6$  + 10 mol-% FeO, we observed a particular behavior of the spectrum with time whilst heating, with a shift of the line position and a pro-

gressive broadening of the line up to 14 minutes of heating (Figure 4). This evolution is then reversed and we observed a decrease of the chemical shift and a narrowing of the peak. This modification appears approximately at the same time as the  $^{19}\text{F}$  signal is observed (Figure 3). These observations support the suggestion of a continuous decrease of the concentration of paramagnetic iron in the sample with FeO caused by evaporation of  $\text{Fe}^{\text{II}}$  compounds from the system.

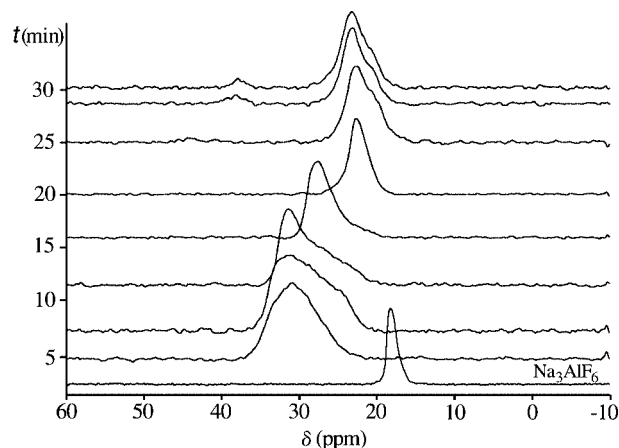


Figure 4. HT  $^{27}\text{Al}$  NMR spectra of  $\text{Na}_3\text{AlF}_6$ -10 mol-% FeO at 1020 °C vs. heating time.

As mentioned above, the calculated value of the  $^{27}\text{Al}$  chemical shift ( $\text{Na}_3\text{AlF}_6$  + 10 mol-% FeO), assuming reaction B and no influence of the unpaired electrons, is  $\delta = 20.6$  ppm. This calculated value is in good agreement with the experimental value of  $\delta = 23.0$  ppm for the sample after 30 minutes of heating.

In the case of  $\text{Fe}_2\text{O}_3$  (after five minutes of heating), the  $^{27}\text{Al}$  chemical shift remains constant during further heating (Figure 5). This observation confirms the presence of stable, nonvolatile fluoride species in the melt involving the  $\text{Fe}^{\text{III}}$  paramagnetic iron nuclei.

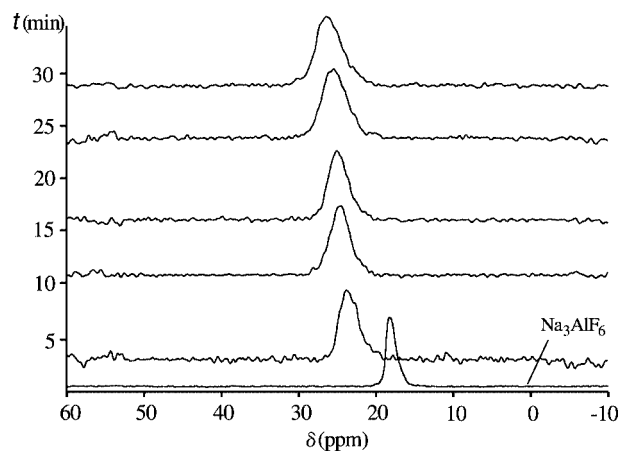


Figure 5. HT  $^{27}\text{Al}$  NMR spectra of  $\text{Na}_3\text{AlF}_6$ -1 mol-%  $\text{Fe}_2\text{O}_3$  at 1020 °C vs. heating time.



## Conclusions

High-temperature NMR experiments have been performed in molten cryolite with addition of different amounts of FeO or Fe<sub>2</sub>O<sub>3</sub>. The selective observation of the <sup>27</sup>Al, <sup>23</sup>Na, and <sup>19</sup>F signals in the melts at 1020 °C and their evolution with increasing iron oxide content has allowed us to confirm the formation of oxofluoroaluminate species. The non-observation of the <sup>19</sup>F signal caused by the paramagnetic influence of the Fe<sup>II</sup> ion in the melt is associated with the formation of “fluorinated iron” species. Even though this paramagnetic effect causes a strong broadening and distortion of the signals, we can still take advantage of this interaction and follow the formation and/or loss of the Fe<sup>II</sup> species. In the Na<sub>3</sub>AlF<sub>6</sub>–FeO melts, the <sup>19</sup>F signal was finally detected after 14 minutes heating, which would coincide with the evaporation of Fe<sup>II</sup> species. However, it was not observed at all in the Na<sub>3</sub>AlF<sub>6</sub>–Fe<sub>2</sub>O<sub>3</sub> system due to the presence of stable, nonvolatile species involving the paramagnetic iron nuclei.

## Experimental Section

Samples were prepared by mixing Na<sub>3</sub>AlF<sub>6</sub> (natural, from Ivigtut) and FeO or Fe<sub>2</sub>O<sub>3</sub> (reagent grade, Aldrich). The compositions ranged from 0 to 14 mol-% of FeO and from 0 to 1 mol-% of Fe<sub>2</sub>O<sub>3</sub> (see Table 1).

All NMR experiments were carried out using a Bruker DSX 400 (9.4 T) NMR spectrometer operating at frequencies of 104.2 MHz for <sup>27</sup>Al, 105.8 MHz for <sup>23</sup>Na, and 376.3 MHz for <sup>19</sup>F. <sup>27</sup>Al, <sup>23</sup>Na, and <sup>19</sup>F chemical shifts are referenced to 1 M aqueous solutions of Al(NO<sub>3</sub>)<sub>3</sub>, NaCl, and CFC<sub>3</sub> at room temperature, respectively. High temperature (HT) NMR experiments were performed using the previously described laser-heated system developed at the CRMHT (Orléans, France).<sup>[13]</sup> Every sample was placed in a high purity boron nitride (Carborundum) crucible tightly closed by a screwed BN cap and placed inside the RF coil, in the center of the cryomagnet. The crucible was then heated with a CO<sub>2</sub> laser beam (λ = 10.6 μm, 120 W). The HT NMR spectra were obtained using single-pulse excitation with 20-, 30-, and 18-μs pulses for <sup>27</sup>Al, <sup>23</sup>Na, and <sup>19</sup>F measurements, respectively. Recycle delays of between 500 ms and 2 s (for <sup>19</sup>F) were used, and 64 scans were measured to obtain a reliable signal-to-noise ratio. The powder mixtures were heated and melted up to 1020 °C. <sup>27</sup>Al, <sup>23</sup>Na, and <sup>19</sup>F NMR spectra were recorded for every composition after 4 min for temperature stabilization. In order to follow the kinetics of the iron oxide dissolution, <sup>27</sup>Al, <sup>23</sup>Na, and <sup>19</sup>F NMR spectra were recorded repeatedly up to 30 min at 1020 °C.

The NMR parameters (chemical shifts, line widths, quadrupolar coupling constants) were fitted to the experimental spectra with the Winfit program.<sup>[21]</sup>

## Acknowledgments

We would like to acknowledge the financial support of the EEC (contract HPMC-CT-2000-00169) in the framework of the Marie Curie training site “high resolution solid/high temperature liquid nuclear magnetic resonance in materials sciences” (Orleans, France), and Slovak Grant Agencies (VEGA-2/4107/23, APVT-51-008104)

- [1] K. Grjotheim, C. Krohn, M. Malinovsky, K. Matiašovský, J. Thonstad, *Aluminium Electrolysis. Fundamentals of the Hall–Héroult Process*, 2nd ed., Aluminium Verlag GmbH, Düsseldorf, **1982**.
- [2] Å. Sterten, P. A. Solli, E. Skybakmoen, *J. Appl. Electrochem.* **1998**, 28, 781–789.
- [3] J. H. Choi, G. W. Suh, Y. H. Paik, *J. Korean Inst. Met. Mater.* **1991**, 29, 1283–1285.
- [4] K. Horinouchi, N. Tachikawa, K. Yamada, “DSA in Aluminium Reduction Cells.” Proc. 1st Int. Symp. Molten Salt Chem. Technology, Kyoto, Japan, **1983**, pp. 66–72.
- [5] Q. B. Diep, Dr. Ing. Thesis, Norwegian University of Science and Technology, Trondheim, **1998**.
- [6] H. G. Johansen, Dr. Ing. Thesis, Norwegian University of Science and Technology, Trondheim, **1975**.
- [7] H. G. Johansen, A. Sterten, J. Thonstad, *Acta Chem. Scand.* **1989**, 43, 417–420.
- [8] T. E. Jentofsen, E. W. Dewing, G. M. Haarberg, J. Thonstad, *Proc. Electrochem. Soc.* **1999**, 99, 473–484.
- [9] T. E. Jentofsen, Dr. Ing. Thesis, Norwegian University of Science and Technology, Trondheim, **2000**.
- [10] C. Bessada, V. Lacassagne, D. Massiot, P. Florian, J.-P. Coutures, E. Robert, B. Gilbert, *Z. Naturforsch., Teil A* **1999**, 54, 162–166.
- [11] V. Lacassagne, C. Bessada, P. Florian, S. Bouvet, B. Ollivier, J.-P. Coutures, D. Massiot, *J. Phys. Chem. B* **2002**, 106, 1862–1868.
- [12] D. F. Shriver, P. W. Atkins, C. H. Langford, *Inorganic Chemistry*, Oxford University Press, Oxford, 2nd edition, **1994**.
- [13] V. Lacassagne, C. Bessada, B. Ollivier, D. Massiot, P. Florian, J.-P. Coutures, *C. R. Acad. Sci. Paris, Ser. IIB* **1997**, 325, 91–98.
- [14] B. Gilbert, G. Mamantov, G. M. Begun, *J. Chem. Phys.* **1975**, 62, 950.
- [15] F. N. Xiang, H. Kvande, *Acta Chem. Scand.* **1986**, A40, 622.
- [16] B. Gilbert, T. Materne, *Appl. Spectrosc.* **1990**, 44, 299.
- [17] H. Zhou, Dr. Ing. Thesis, Norwegian University of Science and Technology, Trondheim, **1991**.
- [18] F. Šimko, V. Daněk, *Chem. Pap.* **2001**, 55, 269–272.
- [19] F. Šimko, Dr. Ing. Thesis, The Institute of Inorganic Chemistry SAS, Bratislava, **2003**.
- [20] G. Scholz, R. Stösser, *J. Fluorine Chem.* **1997**, 86, 31–142.
- [21] D. Massiot, F. Fayon, M. Capron, I. King, S. Le Calvé, B. Alonso, J.-O. Durand, B. Bujoli, Z. Gan, G. Hoatson, *Magn. Reson. Chem.* **2002**, 40, 70–76.

Received: June 9, 2006

Published Online: September 22, 2006